A group theoretical analysis on transition-metal complexes with metal–ligand multiple bonds

Zhenyang Lin and Michael B. Hall

Department of Chemistry, Texas A&M University, College Station, TX 77843 (USA)

CONTENTS

A. INTRODUCTION

Transition-metal complexes with metal–ligand multiple bonds are of considerable interest in inorganic chemistry [1,2]. In addition to their fundamental importance, metal–ligand multiple bonds appear to be involved in a variety of catalytic cycles in metalloenzymes [3]. Most complexes in this class can be formulated as MT_nL_m, where T is a potentially triple-bonding ligand, such as oxo, sufido, nitrido, imido, and alkylidyne, and L is a single σ-bonding ligand. Following several years of significant development in the structural studies, Nugent and Mayer recently compiled these results in a comprehensive review [1]. In an M–T unit, the potentially triple-bonding ligand provides one σ and two π orbitals to interact with metal orbitals. However, it is not always easy to determine the formal M–T bond order since it is influenced by several factors, e.g. total geometry, coordination number and other T ligands. In a statistical study, it was found that metal–oxo bond lengths depend primarily on the formal M–O bond order derived from a simple ligand field theory for octahedral complexes [2].

In this paper, a group theoretical approach will be used to determine the formal bond order and maximum number of d electrons for a large number of MT_nL_m

---

Correspondence to: M. B. Hall, Department of Chemistry, Texas A&M University, College Station, TX 77843, U.S.A.

complexes with different types of geometry. Several similar individual analyses have been done on specific geometries or complexes [4–7], particularly for octahedral complexes. The analyses of the maximum number of d electrons and the formal bond order is particularly useful for rationalizing the close-shell electronic configuration for a variety of metal–ligand multiple bond complexes and explaining the statistical trend of metal–ligand bond lengths [2]. Rather than develop the general aspects of our approach, which are well-known [8], we will develop specific examples and summarize our results at the conclusion.

B. TRIGONAL-PLANAR COMPLEXES, $MT_{3-n}L_n$ $(n=0-2)$

Recently, Schrock and his co-workers [7] reported the synthesis and structure of a 20-electron trigonal-planar osmium imido complex, $Os(NR)_3$, where R is 2,6-$C_6H_3(Pr^i)_2$ and the Os—N—C angles are very close to 180.0°. It can be easily classified as an MT_3 system with a d^2 configuration (formally NR^{2-} ligand). Figure 1 shows a qualitative molecular orbital interaction diagram for an MT_3 complex. In the figure, the s, p and d orbitals of the central metal atom correspond to $2a_1' + 2e' + e'' +$
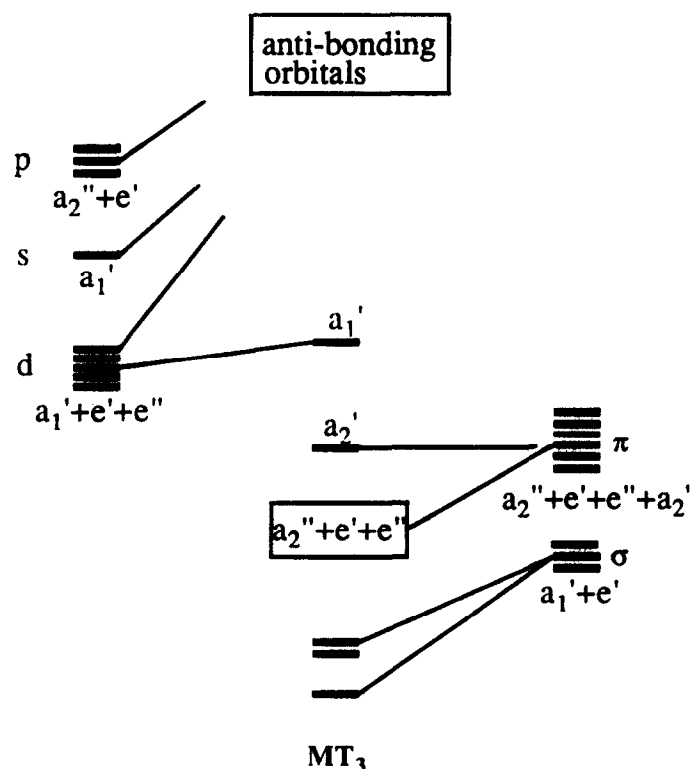

Fig. 1. Orbital interaction diagram for a trigonal-planar MT_3 complex.

a_2'' irreducible representations. The linear combinations of ligand orbitals (one σ and two π for each T) transform as $a_1' + 2e' + e'' + 2a_2'' + a_2'$ in D_{3h} symmetry. The interaction between these two sets from M and T results in a pattern of three σ, five π, and two non-bonding molecular orbitals, one delocalized in the three T ligands and the other localized in the central metal atom, which accommodates two d electrons (see Fig. 1). The a_2' combination from ligand π orbitals cannot find a symmetry-adapted atomic orbital in the central metal atom. Therefore, the central metal atom still conforms an 18-electron configuration since the two extra electrons are localized in the ligands. SCF-Xα-SW calculation on Os(NH)$_3$ gave a similar result [7]. Since there are only five π molecular orbitals in the MT$_3$ complex, we can calculate a formal M–T bond order of 2.67 [$= (3\sigma + 5\pi)/3$].

The above analysis is based on an assumption that metal-p to ligand-p π bonding is comparable with metal-d to ligand-p π bonding, where the metal p orbital (p_π) is perpendicular to the MT$_3$ plane. In most cases, metal p orbitals participate primarily in the metal–ligand σ bonding. In trigonal-planar and square-planar complexes, one p orbital (p_π) involves only π bonding with ligands. Except for trigonal-planar MT$_3$, square-planar MT$_4$ and *trans*-MT$_2$L$_2$ complexes, where the metal p_π and d_π have different symmetry, the metal p_π usually mixes with the metal d_π orbital. Overall interaction is a three-orbital interaction as shown in **A** where two metal orbitals (p_π and d_π) and one ligand's p_π orbital interact. Although the ligand's p_π

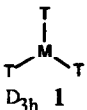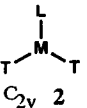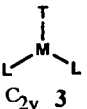Metal   M–T   T Ligand
π-interaction

(A)
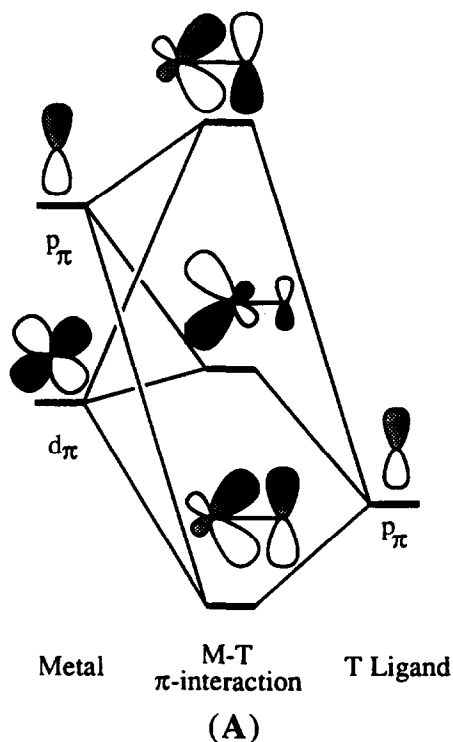
orbital interacts primarily with the metal d_π orbital, the metal d_π–ligand's p_π anti-bonding orbital is significantly stabilized by mixing with the metal p_π orbital. Particularly when a strong π accepting ligand is trans to the T ligand, the occupation of this partially antibonding d_π is very likely. Although the metal-p_π to ligand-p_π interactions for early transition metals are generally weaker than the metal-d_π to lignad-p_π interactions, we prefer the view that the former are sufficiently important that they cannot be neglected. Therefore, the bond order and d-electron counts throughout this paper are based on the above assumption. If one were to take the opposite view, neglect of all metal-p_π to ligand-p_π bonding, the bond order in some cases would decrease.

The analysis of MT_3, above, can also be applied to the orbital interaction of MT_2L (2) and MTL_2 (3). The results are listed in Table 1. Both complexes have a formal bond order of 3.00. The maximum number of d electrons is 4 and 8 for MT_2L and MTL_2, respectively. Early report on the synthesis of d^8 compounds, $(Ph_2PMe)_2M(NR)$ ($R = CF_2CHFCF_3$; $M = Pd$ or Pt) [9(b)], might provide examples for MTL_2 complexes. However, so far no $Pt\equiv NR$ (or $Pd\equiv NR$) complex has been characterized. In Table 1, the irreducible representations with bold text are non-bonding orbitals since either they are free because they do not have a symmetry-adapted orbital partner to interact with, or they are extra since they are left over after completing the metal and ligand interaction. For example, in MT_3 (1) the a_2'

TABLE 1

The irreducible representations of the orbitals of the metal and ligand in a trigonal-planar geometry, $MT_{3-n}L_n$ ($n = 0$, 1 and 2)

Geometry	Irreducible representations				max. M-T bond order (max. b.o.)	max. no. of d electrons for max. b.o.	Examples [References]
	of ligand's		of metal's				
	σ-orbitals	π-orbitals	s+p orbitals	d orbitals			
T | M T T D_{3h} 1	$a_1'+e'$	$a_2''+e''+e'$ $+a_2'$	$a_1'+e'+a_2''$	$e'+e''$ $+a_1'$	2.67	2	Os(NAr)₃ (d²) (Ar: 2,6-C₆H₃(Prⁱ)₂) [7]
L | M T T C_{2v} 2	$2a_1+b_2$	$a_1+a_2+b_1$ $+b_2$	$2a_1+b_1+b_2$	$a_1+b_2+a_2$ $+a_1+b_1$	3.00	4	not found
T | M L L C_{2v} 3	$2a_1+b_2$	b_1+b_2	$2a_1+b_1+b_2$	b_2+ $2a_1+b_1$ $+a_2$	3.00	8	Zr(NR)(NHR)₂ (R: SiBu'₃) * (d⁰) [9a]

*Proposed intermediate.

from ligands cannot find an orbital of the same symmetry on the central metal atom and the a_1' from the central metal atom is an extra one. There are two extra $(a_1 + b_1)$ metal orbitals for the MT_2L (2) complex since the linear combination of the ligand's orbital transform as $3a_1 + 2b_2 + b_1 + a_2$ while the metal orbitals correspond to $4a_1 + 2b_2 + 2b_1 + a_2$ irreducible representations. Four extra metal orbitals $(2a_1 + b_1 + a_2)$ are found for MTL_2 (see Table 1).

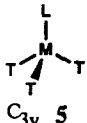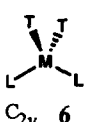## C. FOUR-COORDINATE COMPLEXES, $MT_{4-n}L_n$ ($n = 0$–3)

Metal tetraoxides (or sulfides) are typical examples of MT_4 with tetrahedral structures (4). The linear combinations of the ligand's σ and π orbitals transform as $a_1 + e + 2t_2 + t_1$ and the central metal orbitals as $a_1 + e + 2t_2$. The t_1 combinations from ligands are pure non-bonding since the central metal orbitals do not have t_1 symmetry-adapted representations. The formal M–T bond order is 2.25 ($= (4\sigma + 5\pi)/4$). The maximum number of d electrons corresponds to a d^0 configuration. In addition to numerous examples of d^0 tetraoxides (or sulfides), recent reports on the characterizations of $Os(NBu^t)_4$, $Cr(NBu^t)_4^{2-}$, $Os(NR)O_3$, and $Os(NR)_2O_2$ complexes provide a variety of MT_4 complexes [11] with a d^0 configuration. Several d^1 and d^2 complexes, e.g. MnO_4^{2-}, MnO_4^{3-} and RuO_4^-, are known [12(a)]. The extra d electron(s) occupy M–T π antibonding orbital, and therefore, these complexes are usually very reactive and stable only in strongly basic solutions.

Table 2 lists the results of all other tetrahedral complexes with 3, 2, and 1 potentially triple-bonding ligands. MT_3L (5) has one combination of the ligands' π orbitals free, and a formal bond order of 2.67. MT_2L_2 (6) has no free ligands' π orbital(s) but has an extra metal d orbital (a_1) which can accommodate two d electrons. OsO_2R_2 (d^2) and ReO_2R_2 (d^1) complexes [14] provide examples of filled and half-filled configurations of the a_1 orbital, respectively. MTL_3 (7) has three extra metal orbitals $(a_1 + e)$, and therefore, a maximum d-electron count of 6. A diamagnetic d^4 example, $ReO(MeCCMe)_2Py^+$ [15] (see Table 2), suggests that the orbital energy-level ordering for these three non-bonding orbitals is $e < a_1$. $Os(arene)(NBu^t)$ and $IrCp^*(NBu^t)$ complexes [16] provide excellent examples of full occupation of all three non-bonding orbitals $(a_1 + e$, see Table 2).

Another typical four-coordinate geometry is square-planar. An example of square-planar MT_2L_2 (10) has been reported as the $Os(NAr)_2(PMe_2Ph)_2$ complex [7] which has d^4 configuration and a total of 20 valence electrons. The two extra electrons are delocalized in the ligands' π orbital (b_{2u}). Four d electrons occupy the two non-bonding orbitals $(a_g + b_{1g})$ (see Table 3). Table 3 gives the results of orbital symmetry analyses of this complex together with other complexes which have different numbers of T ligands. Through Tables 2 and 3, one can explain why both isomers 6 and 10 have the same MT_2L_2 formula but do not have same number of metal d electrons (d^2 for 6 and d^4 for 10). A d^4 closed-shell configuration is also predicted from Table 3 for a cis-MT_2L_2 (11).

TABLE 2

The irreducible representations of the orbitals of the metal and ligand in a tetrahedral geometry, $MT_{4-n}L_n$ ($n = 0$–3)

Geometry	Irreducible representations				max. M-T bond order (max. b.o.)	max. no. of d electrons for max. b.o.	Examples [References]
	of ligand's		of metal's				
	σ-orbitals	π-orbitals	s+p orbitals	d orbitals			
T_d 4	$a_1 + t_2$	$e + t_2 + t_1$	$a_1 + t_2$	$e + t_2$	2.25	0	MoO_4^{2-} (d^0) [10a] ReO_4^- (d^0) [10b] ReS_4^- (d^0) [10c] OsO_4 (d^0) [10b]
C_{3v} 5	$2a_1 + e$	$a_1 + 2e + a_2$	$2a_1 + e$	$a_1 + 2e$	2.67	0	MnO_3F (d^0) [12] ReO_3R (d^0) [13] (R: 2,4,6-$C_6H_2Me_3$) $Re(NBu^t)Cl$ (d^0) [20]
C_{2v} 6	$2a_1 + b_1 + b_2$	$a_1 + b_1 + b_2 + a_2$	$2a_1 + b_1 + b_2$	$a_1 + b_1 + b_2 + a_2 + a_1$	3.00	2	OsO_2R_2 (d^2) [14] ReO_2R_2 (d^1) [14] (R: mesityl) CrO_2X_2 (d^0) [12b] (X: halides)
C_{3v} 7	$2a_1 + e$	e	$2a_1 + e$	$e + a_1 + e$	3.00	6	$VOCl_3$ (d^0) [12] $ReO(MeCCMe)_2Py^+$ (d^4) [15] $IrCp^*(NBu^t)$ (d^6) [16] $Os(arene)(NBu^t)$ (d^6) [16]

From Tables 2 and 3, one can see that the maximum number of d electrons can be 6 for mono-T complexes with either tetrahedral or square-planar geometry. Therefore, the early reported d^6 complexes, [9(b)], $(PPh_3)_2M(NR)Cl$ (R = CF_2CHFCF_3; M = Ir or Rh), appear to be the only examples and bear further investigation.

D. FIVE-COORDINATE COMPLEXES, $MT_{5-n}L_n$ ($n = 0$–4)

Similar analyses are employed for both trigonal-bipyramidal and square-pyramidal geometries, and the results are listed in Tables 4 and 5, respectively. Here, we use MT_2L_3 complexes to illustrate our analyses. For a trigonal-bipyramidal complex, ML_5, there are four orbitals (e' and e″) available for π interaction with ligands. The e' orbitals maximize their amplitudes in the equatorial plane while the e″ (pure d) orbitals have maximum amplitude above and below the equatorial plane. For isomer **19** with two axial T ligands, one might have a question on the effective overlap between the ligands' e' and metal's e' orbitals since the metal's e' orbitals

TABLE 3

The irreducible representations of the orbitals of the metal and ligand in a square-planar geometry, $MT_{4-n}L_n$ ($n=0-3$)

Geometry	Irreducible representations				max. M-T bond order (max. b.o.)	max. no. of d electrons for max. b.o.	Examples [References]
	of ligand's		of metal's				
	σ-orbitals	π-orbitals	s+p orbitals	d orbitals			
T T–M–T T D_{4h} 8	$a_{1g}+e_u$ $+b_{1g}$	$a_{2u}+e_g$ $+b_{2g}+$ $a_{2g}+e_u$ $+b_{2u}$	$a_{1g}+e_u$ $+a_{2u}$	e_g+b_{1g} $+b_{2g}$ $+a_{1g}$	2.00	2	not found
T T–M–T L C_{2v} 9	$3a_1+b_2$	a_2 $+2b_1+b_2$ $+a_1*+b_2$	$2a_1+b_1+b_2$	a_1+a_2 $+b_1+b_2$ $+a_1*$	2.33	2	not found
T L–M–L T D_{2h} 10	$2a_g+b_{1u}$ $+b_{2u}$	$b_{3u}+b_{2g}$ $+b_{3g}$ $+b_{2u}$	a_g+b_{1u} $+b_{2u}+b_{3u}$	a_g+b_{2g} $+b_{3g}$ $+a_g+b_{1g}$	2.50	4	$Os(NAr)_2(PMe_2Ph)_2$ (d^4, Ar: 2,6-$C_6H_3(Pr^i)_2$) [7]
T T–M–L L C_{2v} 11	$2a_1+2b_2$	$a_1+b_1+a_2$ $+b_2$	$2a_1+b_2+b_1$	$a_1+a_2+b_2$ $+a_1+b_1$	2.50	4	not found
T L–M–L L C_{2v} 12	$3a_1+b_2$	b_1+b_2	$2a_1+b_2+b_1$	a_1+b_2 $+a_1+b_1$ $+a_2$	3.00	6	$(PPh_3)_2M(NR)Cl$ (d^6, M=Ir or Rh)* [9b]

*Proposed structure.

have δ character with respect to the two T ligands. However, the metal's e′ orbitals are not pure d_δ orbitals. In fact, through d–p mixing, they can overlap weakly with the ligands' e′ (π) combinations. The occupation of these two high-energy (e′) orbitals is very unlikely in an MT_2L_3 (**19**) complex. Therefore, we give a formal M—T bond order of 3.00 with a d^0 configuration for **19** (see also Table 4). For isomers **20** and **21** with two cis T ligands, the four metal orbitals (e′ and e″) can overlap effectively with the ligands' π orbitals. Therefore, both isomers have a formal M—T bond order of 3.00 and a d^0 configuration. Because of the weak π interaction in **19**, examples found for MT_2L_3 complexes adopt isomers **20** and **21** rather than **19** (see Table 4). Those complexes listed as examples for a trigonal-bipyramidal MT_2L_3 (**20**) have a T—M—T angle smaller than 120° (ca. 110°). This result can be explained in the

following manner. Since the two metal d orbitals (e″) which are available for π interaction with ligands are perpendicular to each other, for isomer **20**, the best M–T π overlaps occur when the T–M–T angle is 90°. The π interaction between the metal's e′ and the ligands' orbitals remains roughly unchanged when the T–M–T angle decreases from 120° because the d–p mixing allows a reorganization in the metal's e′ orbitals so that they can maximize their π overlap with the ligands' π orbitals. Therefore, the observed small T–M–T angles for those complexes with

TABLE 4

The irreducible representations of the orbitals of the metal and ligand in a trigonal-bypyramidal geometry, $MT_{5-n}L_n$ ($n=0$–4)
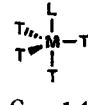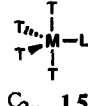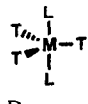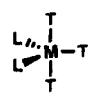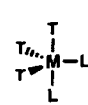
| Geometry | Irreducible representations | | | | max. M-T bond order (max. b.o.) | max. no. of d electrons for max. b.o. | Examples [References] |
| | of ligand's | | of metal's | | | | |
	σ-orbitals	π-orbitals	s+p orbitals	d orbitals			
D_{3h} **13**	$2a_1'+a_2'' +e'$	$e'+e'' \quad a_2''+a_2' +e'+e''$	$a_1'+e' +a_2''$	$a_1'+e' +e''$	1.80	0	not found
C_{3v} **14**	$3a_1+e$	$2e+ a_1+a_2+e$	$2a_1+e$	a_1+2e	2.00	0	OsO_4Cl^- (d⁰) [17a] $OsO_4(NC_7H_{13})$ (d⁰) [17b]
C_{2v} **15**	$3a_1+b_1 +b_2$	$a_1+b_2 +a_2+b_1+ a_1+b_2+ a_2+b_1$	$2a_1+b_1 +b_2$	$2a_1+b_2 +a_2+b_1$	2.00	0	not found
D_{3h} **16**	$2a_1'+a_2'' +e'$	$e'+e'' \quad a_2''+a_2'$	$a_1'+e' +a_2''$	$a_1'+e' +e''$	2.33	0	OsO_3F_2 (d⁰) [18] $RuO_3(OH)_2{}^{2-}$ [32]
C_{2v} **17**	$3a_1+b_1 +b_2$	$b_2+a_2 +b_1+ a1+ b_2+b_1$	$2a_1+b_1 +b_2$	$2a_1+b_2 +a_2+b_1$	2.33	0	not found
C_s **18**	$4a'+a''$	$2a'+2a'' a'+a''$	$3a'+a''$	$3a'+2a''$	2.33	0	ReO_3PyOX (d⁰) (X: ReO_3Py_2) [19]

TABLE 4 (continued)

Geometry	Irreducible representations				max. M-T bond order (max. b.o.)	max. no. of d electrons for max. b.o.	Examples [References]
	of ligand's		of metal's				
	σ-orbitals	π-orbitals	s+p orbitals	d orbitals			
D_{3h} **19**	$2a_1'+a_2''$ $+e'$	$e''+e'$	$a_1'+e'$ $+a_2''$	$a_1'+e''$ $+e'$	3.00	0	not found
C_{2v} **20**	$3a_1+b_1$ $+b_2$	$a_1+b_2+a_2$ $+b_1$	$2a_1+b_1$	$2a_1+b_2$ $+a_2+b_1$	3.00	0	$Re(NBu^t)_2Cl_3$ (d^0) [20] $WO_2[O_2(CMe_2)_2]R$ (d^0, R: CH_2CMe_3) [21]
C_s **21**	$4a'+a''$	$a'+2a''+a'$	$3a'+a''$	$3a'+2a''$	3.00	0	ReO_2Me_3 (d^0) [22]
C_s **22**	$4a'+a''$	$a'+a''$	$3a'+a''$	$2a'+a''$ $+a'+a''$	3.00	4	$VOCl_2(NMe_3)_2$(d^1) [23] $Os(CR)COCl(PPh_3)_2$ (d^4, R: Tol) [24] $Os(CTeMe)(CO)_2L_2^+$ (d^4, L: PPh_3) [25]
C_s **23**	$4a'+a''$	$a'+a''$	$3a'+a''$	$2a'+a''$ $+a'+a''$	3.00	4	$MoOCl(CH_2CMe_3)_3$ (d^0) [26]

conformation **20** result from a balance between steric or σ-bonding effects and maximizing the M—T π interaction.

In Table 5, we summarize our analysis for square-pyramidal geometries. For **30**, **33** and **34**, after taking into account all of the orbital interaction between metal and ligands, one of the extra orbitals (a' or a_1) results from s–p–d mixing and has a maximum amplitude in the vacant position (see (**B**)). This high-energy orbital is unlikely to be occupied with d electrons and is marked by bold type and *.

(B)   **(C)**

For MT_2L_3 (**31**), the two b_2 with bold and superscript * cannot interact with each other since the overlap between them is zero (see (**C**)). The $Os(NAr)_2I_2(PMe_2Ph)$ complex [7] with a d^2 configuration provides an example of MT_2L_3 (**31**) although the N–Os–N angle (151.2°) is less than 180.0°. Since our analysis of a trigonal-bipyramidal structure for MT_2L_3 (**20**) gives a d^0 configuration, we classify the Os complex as a square-pyramidal structure. The small N–Os–N angle is probably a result of steric effects.

TABLE 5

The irreducible representations of the orbitals of the metal and ligand in a square-pyramidal geometry, $MT_{5-n}L_n$ ($n = 0$–4)
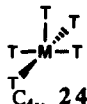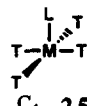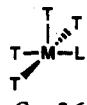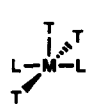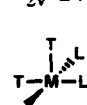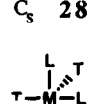
Geometry	Irreducible representations				max. M-T bond order (max. b.o.)	max. no. of d electrons for max. b.o.	Examples [References]
	of ligand's		of metal's				
	σ-orbitals	π-orbitals	s+p orbitals	d orbitals			
C_{4v} **24**	$2a_1+b_1$ $+e$	a_1+e+b_2 $+a_2+b_1$ $+2e$	$2a_1+e$	a_1+e $+b_1+b_2$	1.80	0	not found
C_{4v} **25**	$2a_1+b_1$ $+e$	a_1+e+b_2 $+a_2+b_1$ $+e$	$2a_1+e$	a_1+e $+b_1+b_2$	2.00	0	not found
C_s **26**	$4a'+a''$	$2a'+2a''+$ $2a'+2a''$	$3a'+a''$	$3a'+2a''$	2.00	0	not found
C_{2v} **27**	$3a_1+b_1$ $+b_2$	a_1+a_2+ b_1+b_2+ b_1+b_2	$2a_1+b_1+$ b_2	$2a_1+a_2+$ b_1+b_2	2.33	0	not found
C_s **28**	$3a'+2a''$	$3a'+a''+$ $2a''$	$3a'+a''$	$3a'+2a''$	2.33	0	not found
C_s **29**	$4a'+a''$	$2a'+2a''+$ $a'+a''$	$3a'+a''$	$3a'+2a''$	2.33	0	not found

TABLE 5 (*continued*)

| Geometry	Irreducible representations				max. M-T bond order (max. b.o.)	max. no. of d electrons for max. b.o.	Examples [References]
	of ligand's		of metal's				
	σ-orbitals	π-orbitals	s+p orbitals	d orbitals			
 C_s **30**	$3a'+2a''$	$2a'+a''$ $+a''$	$3a'+a''$	$2a'+2a''$ $+a'$ *	2.50	0	not found
 C_{2v} **31**	$3a_1+b_2$ $+b_1$	$a_1+a_2+b_1$ $+b_2$ *	$2a_1+b_1+b_2$	$2a_1+b_1$ $+a_2+$ $+b_2$ *	2.50	2	$Os(NAr)_2I_2PMe_2Ph$ $(d^2,$ Ar: $2,6\text{-}C_6H_3Pr_2^i)$ [7]
 C_s **32**	$4a'+a''$	$2a'+2a''$	$3a'+a''$	$3a'+2a''$	3.00	0	not found
 C_{4v} **33**	$2a_1+e+b_1$	e	$2a_1+e$	$e+b_1$ $+a_1$*$+b_2$	3.00	2	$Mo(N)Cl_4^-$ (d^0) [27] $Tc(N)Br_4^-$ (d^1) [28] $ReOCl_4^-$ (d^2) [29] $Os(NMe)R_4$ (d^2)[30]
 C_s **34**	$4a'+a''$	$a'+a''$	$3a'+a''$	$2a'+a''$ $+a'$*$+a''$	3.00	2	not found

Combining estimates of π-overlaps, steric effects, and the trans influence, we predict the most stable structure for $MT_{5-n}L_n$ ($n=2\text{--}4$) complexes as follows:

	Close-shell d configuration	Most stable structure(s)
MT_3L_2	d^0	**16** and **18**
MT_2L_3	d^0	**20**
	d^2	**31**
MTL_4	d^4	**22**
	d^2	**33**

The d^2 $ReO_2I(PPh_3)_2$ complex [31] appears to have an intermediate structure between a trigonal-bipyramidal (**20**) and a square-pyramidal (**31**) with an O—Re—O

angle of 138.7°. When one considers it as a trigonal-bipyramidal structure (**20**), the two d electrons should occupy a metal–ligand π antibonding orbital (see Table 4). When one views it as a square-pyramidal structure (**31**), the two d electrons occupy in a non-bonding d orbital (see Table 5). The above discussion indicated that most complexes with conformation **20** have a small T–M–T angle, ca. 110°, while the representative of conformation **31** has a T–M–T angle of 151.2°. From these results, we can see that the geometry of the Re complex is close to conformation **31** but retains some characteristics of conformation **20**. Therefore, the two d electrons must occupy an orbital with weak Re–O π antibonding character. Occupying this orbital results in an Re–O bond distance (1.742 Å) that is longer than that in the ReO_4^- complex (1.719 Å) [10] with a bond order of only 2.25, but shorter than the mean Re–O distance (1.761 Å) in *trans*-ReO_2L_4 complexes, which have a d^2 configuration and a bond order of 2.00. The latter is unique since almost all complexes with the M–T π antibonding orbital(s) occupied have the longest M–T bond distance (see discussion later).

The d^2 complex $RuO_3(OH)_3^{2-}$ [32] with structure **16** was reported to have long Ru–O bonds (1.75–1.76 Å). As we can see from Table 4, an MT_3L_2 complex with structure **16** prefers a d^0 close-shell configuration and formal bond order of 2.33. The long Ru–O bond distance, compared with the Ru–O bond distances of 1.705 Å in RuO_4 (bond order 2.25) and of 1.705–1.726 Å in *trans*-RuO_2L_4 (bond order 2.00) [33], must result from the two d electrons occupying M–T π antibonding orbital(s).

From Tables 4 and 5, the maximum number of d electrons for five-coordinate complexes, MTL_4, is 4. Therefore, an early report on the existence of d^6 complexes [9(b)], e.g. $(PPh_3)_2Ir(CO)Cl(NR)$ and $(PPh_3)_2M(CO)_2(NR)$ ($R = CF_2CHFCF_3$; M = Ru or Os), are unlikely to be true.

E. OCTAHEDRAL COMPLEXES, $MT_{6-n}L_n$ ($n = 0–5$)

The results of our analyses on octahedral complexes are given in Table 6. In an octahedral complex, there are three metal d orbitals of π symmetry (t_{2g} set). Complexes with metal–ligand multiple bonds usually adopt structures such as **40** for fac-MT_3L_3, **41** for *trans*-MT_2L_4, **42** for *cis*-MT_2L_4, and **43** for MTL_5. Simple bonding descriptions can be found in the literature for these four common structures [3–7]. In a fac-MT_3L_3 complex, the three d orbitals interact with the $p_π$ combinations of T ligands and M–T bond is formally a double bond. In a *cis*-MT_2L_4 complex, the formal M–T bond order is 2.5 since three d orbitals are shared among two T ligands. In a trans-MT_2L_4 complex, one d orbital is purely non-bonding because it does not overlap with the ligands' π orbitals, giving an M–T formal bond order of 2.00. This formal bond order cannot be used to relate the M–T bond distance because the trans influence significantly lengthens some M–T bond distances. Thus, the M–T bond in the *trans*-MT_2L_4 complexes is one of the longest bonds among

complexes containing the same M and T ligand(s), which conform to the d configurations listed in Tables 1–6. In an MTL_5 (43) complex, two of the t_{2g} orbitals interact with the two p_π orbitals, giving a formal bond order of three and a d^2 configuration. Most complexes with one potential triple-bonding ligand adopt this structure (43). These arguments have been used to explain the statistical observation on the general trend of metal–oxo bond lengths, monooxo (3.0) < cis-dioxo (2.5) < fac-trioxo (2.0) < trans-dioxo (2.0) (number in parentheses is the formal bond order) [2].

From Table 6, we can see that the maximum number of d electrons in octahedral

TABLE 6

The irreducible representations of the orbitals of the metal and ligand in an octahedral geometry, $MT_{6-n}L_n$ ($n = 0-5$)
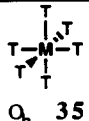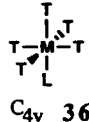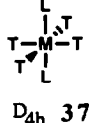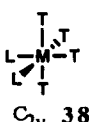
| Geometry | Irreducible representations | | | | max. M-T bond order (max. b.o.) | max. no. of d electrons for max. b.o. | Examples [References] |
| | of ligand's | | of metal's | | | | |
	σ-orbitals	π-orbitals	s+p orbitals	d orbitals			
O_h 35	$a_{1g}+e_g+t_{1u}$	$t_{2g}+t_{1u}+t_{1g}+t_{2u}$	$a_{1g}+t_{1u}$	e_g+t_{2g}	1.50	0	not found
C_{4v} 36	$3a_1+b_1+e$	$e+b_2+a_2+b_1+a_1+2e$	$2a_1+e$	$a_1+e+b_1+b_2$	1.60	0	not found
D_{4h} 37	$2a_{1g}+e_u+a_{2u}+b_{1g}$	$b_{2g}+e_g+a_{2u}+a_{2g}+b_{2u}+e_u$	$a_{1g}+e_u+a_{2u}$	$e_g+b_{2g}+b_{1g}+a_{1g}$	1.75	0	not found
C_{2v} 38	$3a_1+2b_1+b_2$	$a_1+b_1+b_2+a_1+2b_1+a_2+b_2$	$2a_1+b_1+b_2$	$2a_1+a_2+b_1+b_2$	1.75	0	$[Os(O)_4(OH)_2]^{2-}$ (d^0) [34]
C_{2v} 39	$4a_1+b_1+b_2$	$a_1+b_1+b_2+a_1+b_2+b_1$	$2a_1+b_1+b_2$	$2a_1+a_2+b_1+b_2$	2.00	0	not found
C_s 40	$5a'+a''$	$a'+2a''+2a'+a''$	$3a'+a''$	$3a'+2a''$	2.00	0	$MoO_3(dien)$ (d^0) [35] $ReO_3Cl_3^{2-}$ (d^0) [36] ReO_3Cp (d^0) [37]

162   Z. Lin and M.B. Hall/Coord. Chem. Rev. 123 (1993) 149–167

TABLE 6 (continued)

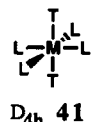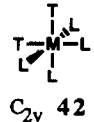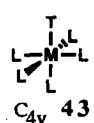| Geometry	Irreducible representations				max. M-T bond order (max. b.o.)	max. no. of d electrons for max. b.o.	Examples [References]
	of ligand's		of metal's				
	σ-orbitals	π-orbitals	s+p orbitals	d orbitals			
D_{4h} 41	$2a_{1g}+e_u$ $+b_{1g}+a_{2u}$	e_g+ $+e_u$	$a_{1g}+e_u+a_{2u}$	$a_{1g}+e_g$ $+b_{1g}+$ $+b_{2g}$	2.00	2	$MoO_2(CN)_4^{2-}$ (d²) [38] $OsO_2Cl_4^{2-}$ (d²) [39]
C_{2v} 42	$3a_1+b_1$ $+2b_2$	a_1+a_2+ $+b_1+b_2$	$2a_1+b_1+b_2$	$2a_1+a_2$ $+b_1+b_2$	2.50	0	$MoO_2F_4^{2-}$ (d⁰) [40]
C_{4v} 43	$3a_1+e+b_1$	e	$2a_1+e$	a_1+e+b_1 $+b_2$	3.00	2	$Ta(NPh)Cl_3(THF)PEt_3$ (d⁰) [41a] [41b] $MoOCl_2(PMePh_2)_3$ (d¹) $Re(N)Cl_5^{2-}$ (d²) [42]

complexes with M—T bond(s) is 2. In d⁴ complexes, such as some iron- and ruthenium-oxo complexes [33], two electrons occupy metal—oxygen π antibonding orbitals. This results in substantially longer M—O bonds. For example, the Ru—O bond distance in $RuOL_5$ (43) complexes with d⁴ configurations ranges from 1.765 Å to 1.826 Å, while it is 1.705–1.726 Å in d² trans-RuO_2L_4 complexes and 1.705 Å in RuO_4 [33].

F. COMPLEXES WITH HIGHER COORDINATION NUMBERS

Since the number of available metal orbitals is 9, complexes with formula of $MT_{9-n}L_n$ (0 < n < 8) are unlikely to exist. An 8-coordinate complex with only one T ligand, MTL_7, is possible since the formal M—T bond order can reach 2.00. A recent report on the structures of $Cp_2^*Ta(H)(O)$, $Cp_2^*Ta(H)(NC_6H_5)$, $Cp_2^*Zr(py)(S)$, and $Cp_2Zr(THF)(NBu^t)$ complexes [43] provides examples of 8-coordinate complexes with a potentially triple bonding ligand. All these complexes have the general formula, Cp_2MTL, with formal M—T bond order of 2.00. For a V-shape Cp_2M fragment with a pseudo-C_{2v} symmetry, where each Cp ligand acts like a three-electron pair σ-donor, the linear combinations of the six σ-donating orbitals of Cp transform as $2a_1+b_1+2b_2+a_2$ irreducible representations while the transition-metal's s, p and d orbitals span $4a_1+2b_1+2b_2+a_2$. The interaction between the orbitals of the metal and the two orbitals of the Cp ligands results in three extra metal orbitals ($2a_1+b_1$)

available for interaction with other ligands. Among these three extra orbitals, only the b_1 orbital, which has maximum amplitudes in a plane perpendicular to the Ct–M–Ct plane (Ct = centroid of the Cp ligand), has π-bonding symmetry. Therefore, for Cp_2MTL complexes, where the T–M–L plane is perpendicular to the Ct–M–Ct plane, the M–T π bonding electron density must lie on the L–M–T plane. Because of the unique nature of the three available frontier orbitals of Cp_2M fragment, structures **D** instead of **E** were usually written in the literature [43(d)]. The extra π bonding orbital of the oxygen ligand in **E** is perpendicular to the O–Zr–C plane and cannot find a matching symmetry-adapted orbital on the Cp_2Zr fragment.

(D)   **(E)**
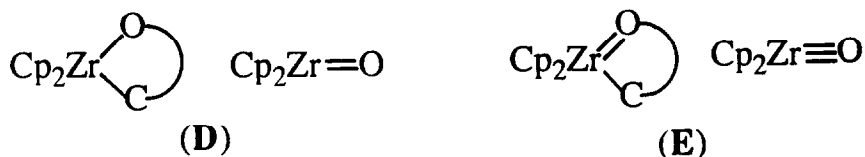
A few 7-coordinate complexes with one T ligand have been reported [33]. The most common structure is pentagonal-bipyramidal with the T ligand occupying one of the two axial positions. The two p_π orbitals of the T ligand interact with the two d orbitals (d_{xz}, d_{yz}) to form M–T triple bonds ($1\sigma + 2\pi$) and to have a d^0 configuration. For example, d^0 $Mo(T)L_2(S_2CNEt_2)_2$ (L = Cl and Br, and T = O and NPh) complexes [44(a), (b)] have a pentagonal-bipyramidal structure with the T ligand occupying one of the two axial positions.

Capped octahedral complexes, $(Nb(E)Cl_3PMe_3)_3$ (E = O and S) [45], were also reported. Beginning with an octahedral complex, we can define the three t_{2g} non-bonding orbitals with respect to the C_3 axis as:

$$t_{2g}(O_h): \begin{cases} d_{z^2} & a_1(C_{3v}) \\ (2/3)^{1/2}d_{x^2-y^2}+(1/3)^{1/2}d_{xz} \\ (2/3)^{1/2}d_{xy}-(1/3)^{1/2}d_{yz} \end{cases} e(C_{3v})$$

The capping T ligand then interacts with the a_1 orbital to form a σ-bond, and weakly overlaps with the e orbitals to form two π-bonds. A distortion away from a regular octahedron, i.e. opening of the capped triangular face, leads to much stronger M–T π interaction. Again, a d^0 configuration is expected for capped octahedral MTL_6 complexes.

G. BOND ORDER AND BOND DISTANCE

Before going into the details of the bond length and bond order relationship, we comment here on those oxo complexes which have an exceptionally long metal–oxo bond distance. Usually, *trans*-dioxo octahedral complexes (**41**) have much

longer M—O bonds than fac-trioxo complexes (40), although both have the same formal bond order (2.0). This phenomenon is explained by the large trans influence of the oxo group, i.e. a difference in the σ bonding. Some other complexes have very long M—O bond lengths because the M—O π-antibonding orbital(s) is occupied, i.e. the metal d electrons exceed the maximum number of d electrons listed in Tables 1–6. From a traditional point of view, the M—O formal bond order is reduced by 1 when two electrons occupy metal–ligand π-antibonding orbital(s). However, modern orbital interaction models predict that the antibonding orbital is destabilized more than the corresponding bonding one is stabilized. This implies that the occupation of metal–ligand π-antibonding orbital(s) will increase the M—O bond distance significantly, and the formal bond order calculated in the traditional way will not predict the bond distance. Unusually long metal—oxo bonds have also been reported in some complexes which have the same composition and structure but differ only in the M—O bond lengths. This phenomenon was termed as "distortional isomerism" [46] or "bond stretch isomerism" [47]. Most recently, both theoretical and experimental examinations disprove the existence of an isomer with a long Mo—O bond in cis-mer-MoOCl$_2$(PR$_3$)$_3$ complexes, and now "bond stretch isomerism" is a controversial topic [48,49]. In summary, all these complexes with exceptionally long M—O bonds are not included in the following discussion since the formal bond order cannot reflect the trend of metal—ligand bond lengths.

As mentioned in the introduction, the factors that influence the individual metal—ligand multiple bond distance are not simple. However, the formal bond order is possibly one main factor that can be used to explain the statistical trends (not individuals) of M—O bond lengths for different metal—oxo complexes. Its usefulness will be examined through examples listed in Table 7. In the table, we use statistical data [2] as much as possible. If no statistical data can be found, a range of bond distances is given when more than one example is found. In the list of Os imido complexes, the Os—NR bond distances are compared for those complexes with same R group since we found that comparison between Os—NR distances with different R groups is inconsistent. We can see from Table 7 that the trend of M—T bond lengths is clearly related to the formal bond order. An exception is seen for MoO$_4^{2-}$, which has the longest Mo—O bond although the formal bond order is greater than 2.

In the previous statistical study [2], it was found that the M—O bond lengths in mono-oxo complexes do not show a significant oxidation-state dependence and exhibit only a slight dependence on coordination number. This observation can be easily explained from the above discussions since all mono-oxo complexes have a formal bond order of 3.00 regardless of oxidation state and coordination number. It was also shown that the average M—O bond length in mono-oxo complexes decreases gradually on moving from left to right across the Periodic Table. This trend is not difficult to understand if the M—O bond lengths primarily depend on the formal bond order. The gradual decrease of the average M—O bond length is a result of the

TABLE 7

Metal–ligand multiple bond distances of some selected complexes

Complexes	Geometry	d^n	Bond order	M–T distance (Å)	Comments [References]
$OsO_4(OH)_2^{2-}$	**38**	d^0	1.75	1.750	[34]
$OsO_2L_4(trans)$	**41**	d^2	2.00	1.742	Mean [2]
OsO_4L	**14**	d^0	2.00	1.690–1.722	$L = Cl^-$ and NC_7H_{13} [17]
OsO_4	**4**	d^0	2.25	1.684–1.711	[10]
OsO_2R_2	**6**	d^2	3.00	1.695	R = mesityl [14]
$OsOL_4$	**33**	d^2	3.00	1.630–1.670	[33]
$Os(NAr)_2L_2$	**10**	d^4	2.50	1.790	$L = PMe_2Ph$ [7]
$Os(NAr)_2I_2L$	**31**	d^2	2.50	1.770	$L = PMe_2Ph$ [7]
$Os(NAr)_3$	**1**	d^2	2.67	1.736	[7]
$Os(O)(NAr)L_2$	**6**	d^2	3.00	1.710	$L = NAr(CH_2)_2ArN$ [7]
$ReO_2L_4(trans)$	**41**	d^2	2.00	1.761	Mean [2]
$ReO_3L_3(fac)$	**40**	d^0	2.00	1.690–1.720	See Fig. 3 in ref. 2
ReO_4^-	**4**	d^0	2.25	1.721	[10]
ReO_3L	**5**	d^0	2.67	1.690–1.702	$L = Cl^-$ and $C_6H_2Me_3$ [13,33]
ReO_2R_2	**6**	d^1	3.00	1.688	$R = C_6H_2Me_3$ [14]
Re mono-oxo		d^{1-2}	3.00	1.686	mean [2]
$MoO_2(CN)_4^{2-}$	**41**	d^2	2.00	1.828	[38]
Mo fac-trioxo	**40**	d^0	2.00	1.726	Mean [2]
MoO_4^{2-}	**4**	d^0	2.25	1.760	[9]
Mo cis-dioxo	**42**	d^0	2.50	1.704	Mean [2]
Mo mono-oxo	**43**	d^2	3.00	1.681	Mean [2]
Mo mono-oxo	**33**	d^2	3.00	1.669	Mean [2]

periodic decrease in the size of the transition metal atom. It should be noted here that the formal bond order cannot be used to explain the M–T bond distance ordering for individual complexes since the magnitude of M–T π overlap and the σ bonding are different for different geometries (in this simple analysis, we assume each M–T π overlap is equivalent to a π bond and that all σ bonds are equal).

H. CONCLUSION

The above discussion indicates that the statistical trend of M–T bond distances is closely related to the formal M–T bond order obtained from a simple group theoretical analyses. Most transition metal complexes with potentially triple-bonding ligand(s) conform to the maximum number of d electrons listed in Tables 1–6. A small number of complexes with d electron configurations larger than the maximum

number of d electrons listed in Tables 1–6 have significantly longer M—T bond distances since the metal–ligand π antibonding orbitals are occupied.

REFERENCES

1 W.A. Nugent and J.M. Mayer, Metal–Ligand Multiple Bonds, Wiley-Interscience, New York, 1988.
2 J.M. Mayer, Inorg. Chem., 27 (1988) 3899.
3 (a) J. Chatt, L.M. da Camara Pina and R.L. Richards, New Trends in the Chemistry of Nitrogen Fixation, Academic Press, London, 1980.
   (b) G. Spiro, Molydenum Enzymes, Wiley-Interscience, New York, 1985.
4 J.M. Mayer, D.L. Thorn and T.H. Tulip, J. Am. Chem. Soc., 107 (1985) 7454.
5 D.C. Brower, J.L. Templeton and D.M.P. Mingos, J. Am. Chem. Soc., 109 (1987) 5203.
6 (a) J.W. Lauher and R. Hoffmann, J. Am. Chem. Soc., 98 (1976) 1729.
   (b) K. Tatsumi and R. Hoffmann, Inorg. Chem., 19 (1980) 2656.
   (c) D.M.P. Mingos, J. Organomet. Chem., 179 (1979) C29.
7 M.H. Schofield, T.P. Kee, J.T. Anhaus, R.R. Schrock, K.H. Johnson and W.M. Davis, Inorg. Chem., 30 (1991) 3595.
8 T.A. Albright, J.K. Burdett and M.H. Whangbo, Orbital Interactions in Chemistry, Wiley, New York, 1985.
9 (a) C.C. Cummins, S.M. Baxter and P.T. Wolczanski, J. Am. Chem. Soc., 110 (1988) 8731.
   (b) M.J. McGlinchey and F.A.G. Stone, Chem. Commun., (1970) 1265.
10 (a) B.M. Gatehouse and P. Leverett, J. Chem. Soc. A, (1969) 849.
   (b) B. Krebs and K.D. Hasse, Acta. Crystallogr. Sect. B, 32 (1976) 1334.
   (c) Y. Do, E.D. Simhon and R.H. Holm, Inorg. Chem., 24 (1985) 4635.
11 (a) A.A. Danapoulos and G. Wilkinson, Polyhedron, 9 (1990) 1009.
   (b) W.A. Nugent, R.L. Harlow and R.J. McKinney, J. Am. Chem. Soc., 101 (1979) 7265.
12 (a) F.A. Cotton and G. Wilkinson, Advanced Inorganic Chemistry, Wiley, New York, 1988, pp. 666, 698.
   (b) A.F. Well, Structural Inorganic Chemistry, Clarendon Press, Oxford, 1984, p. 483.
13 W.A. Herrmann, M. Ladwig, P. Kiprot and J. Riede, J. Organomet. Chem., 371 (1988) C13.
14 P. Stravropoulos, P.G. Edwards, T. Behling, G. Wilkinson, M. Motevalli and M.B. Hursthouse, J. Chem. Soc. Dalton Trans., (1987) 169.
15 J.M. Mayer, T.H. Tulip, J.C. Calabrese and E. Valencia, J. Am. Chem. Soc., 109 (1987) 157.
16 (a) D.S. Clueck, J. Wu, F.J. Hollander and R.G. Bergman, J. Am. Chem. Soc., 113 (1991) 2043.
   (b) R.I. Michelman, R.A. Anderson and R.G. Bergman, J. Am. Chem. Soc., 113 (1991) 5100.
17 (a) R. Weber, K. Dehnicke, U. Müller and D. Fenske, Z. Anorg. Allg. Chem., 516 (1984) 214.

(b) W.P. Griffith, A.C. Skapski, K.A. Woode and M.J. Wright, Inorg. Chim. Acta, 31 (1978) L413.

18 I.R. Beattie, H.E. Blayden, R.A. Crocombe, P.J. Jones and R.S. Odgen, J. Raman Spectrosc., 4 (1976) 313.

19 J.W. Johnson, J.F. Brody, G.B. Ansell and S. Zentz, Acta. Crystallogr. Sect. C, 40 (1984) 2024.

20 A.A. Danapoulos, C.J. Longley, G. Wilkinson, B. Hussain and M.B. Hursthouse, Polyhedron, 8 (1989) 2657.

21 I. Feinstein-Jaffe, J.C. Dewan and R.R. Schrock, Organometallics, 4 (1985) 1189.

22 K. Mertis and G. Wilkinson, J. Chem. Soc. Dalton Trans., (1976) 1488.

23 J.E. Drake, J. Vekris and J.S. Wood, J. Chem. Soc. A, (1968) 1000.

24 G.R. Clark, K. Marsden, W.R. Roper and L.J. Wright, J. Am. Chem. Soc., 102 (1980) 6570.

25 W.R. Roper, J. Organomet. Chem., 300 (1986) 167.

26 J.R.M. Kress, J.M. Russell, M.G. Wesolek and J.A. Osborn, J. Chem. Soc. Chem. Commun., (1980) 431.

27 U. Müller, E. Schweda and J. Strähle, Z. Naturforsch., 388 (1983) 1299.

28 M. Melnik and J.E. Van Lier. Coord. Chem. Rev., 77 (1987) 275.

29 T. Lis and B. Jezowska-Trzebiatowska, Acta. Crystallogr. Sect. B, 33 (1977) 1248.

30 R.W. Marshman and P.A. Shapley, J. Am. Chem. Soc., 112 (1990) 8369.

31 G.F. Ciani, G. D'Alfonso, P.F. Romiti, A. Sironi and M. Freni, Inorg. Chim. Acta, 72 (1983) 29.

32 G. Nowogrocki, F. Abraham, J. Trehoux and D. Thomas, Acta. Crystallogr., 32 (1976) 2413.

33 W.A. Nugent and J.M. Mayer, Metal–Ligand Multiple Bonds, Wiley-Interscience, New York, 1988, Table 5.2.

34 G. Wilkinson, Comprehensive Coordination Chemistry, Vol. 4, Pergamon Press, Oxford, 1987, pp. 591–592 and references cited therein.

35 F.A. Cotton and R.C. Elder, Inorg. Chem., 3 (1964) 397.

36 T. Lis, Acta. Crystallogr. Sect. C, 39 (1983) 961.

37 W.H. Herrmann, M. Taillefer, C. de M. de Bellefon and J. Behm, Inorg. Chem., 30 (1991) 3247.

38 V.M. Day and J.L Hoard, J. Am. Chem. Soc., 90 (1968) 3374.

39 F.H. Kreuse, Acta. Crystallogr., 14 (1961) 1035.

40 B. Spivak and Z. Dori, Coord. Chem. Rev., 17 (1975) 99.

41 (a) M.J. Churchill and H.J. Wasserman, Inorg. Chem., 21 (1982) 223.
   (b) F.A. Cotton, M.P. Diebold and W.J. Roth, Inorg. Chem., 26 (1987) 2848.

42 E. Shustorovich, M.A. Porai-Koshits and Yu.A. Buslaev, Coord. Chem. Rev., 17 (1975) 1.

43 (a) G. Parkin, A. van Asselt, D.J. Leahy, L. Whinnery, N.G. Hua, R.W. Quan, L.M. Henling, W.P. Schaefer, B.D. Santarsiero and J.E. Bercaw, Inorg. Chem., 31 (1992) 82.
   (b) M.J. Carney, P.J. Walsh and R.G. Bergman, J. Am. Chem. Soc., 112 (1990) 6426.
   (c) P.J. Walsh, F.J. Hollander and R.G. Bergman, J. Am Chem. Soc., 110 (1988) 8729.
   (d) M.J. Carney, P.J. Walsh, F.J. Hollander and R.G. Bergman, J. Am Chem. Soc., 111 (1989) 8751.

44 (a) J. Dirand, L. Richard and R. Weiss, J. Chem. Soc. Dalton Trans., (1976) 278.
   (b) E.A. Maatta, B.L. Haymore and R.A.D. Wentworth, Inorg. Chem., 19 (1980) 1055.

45 A. Bashall, V.C. Gibson, T.P. Kee, M. McPartlin, O.B. Robinson and A. Shaw, Angew. Chem. Int. Ed. Engl., 30 (1991) 980.

46 J. Chatt, L. Manojlovic-Muir and K.W. Muir, J. Chem. Soc. Chem. Commun., (1971) 655.

47 Y. Jean, A. Lledos, J.K. Burdett and R. Hoffmann, J. Am. Chem. Soc., 110 (1988) 4506.

48 J. Song and M.B. Hall, Inorg. Chem., 30 (1991) 4433.

49 K. Yoon, G. Parkin and A.L. Rheingold, J. Am. Chem. Soc., 113 (1991) 1437.